

Effects of Geometric and Material Non-linearities on the Tunable Bandgaps and Low-frequency Directionality of Phononic Crystals

Pai Wang,¹ Jongmin Shim,¹ and Katia Bertoldi^{1,2}

¹*School of Engineering and Applied Sciences, Harvard University, Cambridge, Massachusetts 02138, USA*

²*Kavli Institute, Harvard University, Cambridge, Massachusetts 02138, USA*

(Dated: 4th March 2013)

We investigate the effects of geometric and material non-linearities introduced by deformation on the dynamic response of two dimensional phononic crystals. Our analysis not only shows that deformation can be effectively used to tune the bandgaps and the directionality of the propagating waves, but also reveals how geometric and material non-linearities contribute to the tunable response of phononic crystals. Our numerical study provides a better understanding of the tunable response of phononic crystals and opens avenues for the design of systems with optimized properties and enhanced tunability.

PACS numbers: Valid PACS appear here

Phononic crystals (i.e. periodic structures composed of multiple materials with contrast in mechanical properties) have attracted considerable interest due to their ability to tailor the propagation of waves through bandgaps, frequency ranges in which the propagation of sound and elastic waves is forbidden [1–5]. This fundamental property has been recently exploited to design waveguides [6], frequency modulators [7], noise-reduction devices [8] and vibration isolators [9]. It has also been recognized that phononic crystals are characterized by directional behavior that can be exploited to steer or redirect waves in specific directions [3, 10, 11]. The directionality is determined by the level of anisotropy of the structure and can be fully controlled through proper arrangement of the material distribution at the unit cell level [12]. Furthermore, many previous studies have focused on the high frequency propagation directionality of phononic crystals [13–15], while the strongly directional behavior in the low frequency regime is not fully explored despite important potential applications in broadband situations [12].

Motivated by technological applications, a number of studies investigated the effects of both material properties (i.e. contrast in density, Young’s modulus and Poisson’s ratio) [16, 17] and geometry (i.e. volume fraction and topology) [18, 19] on the characteristics of phononic crystals. However, in all these investigations the bandgaps and the directionality of the propagating waves are limited to specific values that cannot be tuned after the manufacturing process. New strategies are required to design phononic crystals with adaptive properties that can be reversibly tuned.

It has been recently demonstrated that mechanical loading can be used as a robust mechanism for *in-situ* tunability of soft and highly deformable 2D phononic crystals [5]. It was shown that both the position and width of the bandgap are strongly affected by the applied deformation [5, 20, 21]. However, the effect of deformation on the directionality of the propagating

waves in the low frequency regime has never been explored. Finally, although it is evident that the applied deformation induces both strong geometric and material non-linearities [5], it is not clear how these two factors contribute to the tunability of the response. To shed light on these important points, here we investigate not only the effect of the applied deformation on the low frequency directionality of the propagating waves, but also the contributions of geometric and material non-linearities to the tunable response of soft phononic crystals. The numerical analyses performed in this study offer a better understanding of the tunable response of phononic crystals and provide guidelines for the design of structures with optimized properties and enhanced tunability.

Here, we focus on two dimensional (2D) soft phononic crystals. Although our analysis is general and can be applied to any architecture, in this study we present numerical results for a square array of circular holes characterized by an initial void volume fraction $V_0 = 60\%$ (Fig. 1A). Here, V_0 is defined as the volume of the voids divided by the total

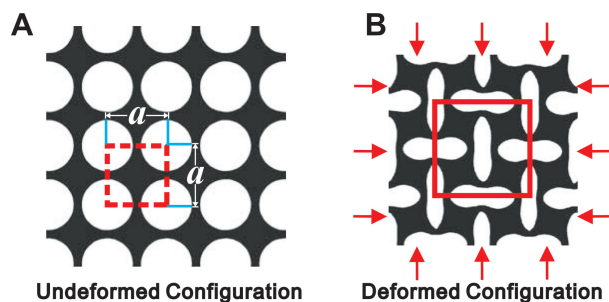


Figure 1: Geometry reorganization induced by instability in a soft phononic crystal comprising a square array of circular holes subjected to equibiaxial compression. The dashed square of size $a \times a$ in (A) indicates the primitive unit cell in the undeformed configuration. The solid square in (B) represents the enlarged representative volume element in the deformed configuration.

volume of the phononic crystal. The non-linear finite-element code ABAQUS/STANDARD is used to deform the structures as well as to investigate the propagation of small-amplitude elastic waves in the pre-deformed phononic crystal. Detailed description of the general formulation and the numerical simulations are provided in the Supplementary Materials [22].

For all the analyses, 2D finite element models are constructed and the accuracy of the mesh is ascertained through a mesh refinement study. We focus on a phononic crystal made of an almost-incompressible elastomeric material whose response is captured by a Gent model [23] characterized by the following strain energy density function:

$$W(I_1, J) = -\frac{G}{2}J_m \log\left(\frac{J_m - (I_1 - 3)}{J_m}\right) - G \log(J) + \left(\frac{K}{2} - \frac{G}{J_m}\right)(J - 1)^2, \quad (1)$$

where $I_1 = \text{trace}(\mathbf{F}^T \mathbf{F})$, $J = \det(\mathbf{F})$, \mathbf{F} denotes the deformation gradient, G and K are the initial shear and bulk moduli and J_m denotes a material constant related to the strain at saturation. We note that the strain energy tends to infinity as $I_1 - 3$ approaches J_m .

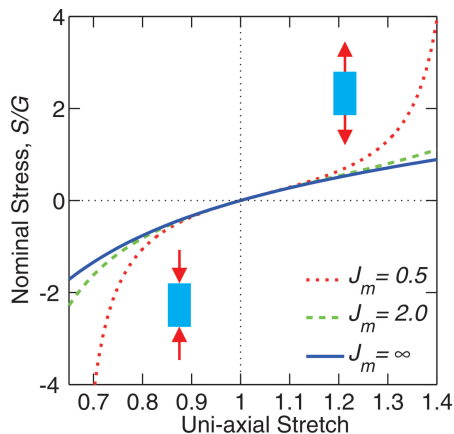


Figure 2: Uniaxial stress-stretch response of a nearly incompressible Gent material with $J_m = 0.5, 2.0$ and ∞ (the last corresponding to a Neo-Hookean material).

Here, we consider an elastomeric material with $G = 1.08 \times 10^6 \text{ N/m}^2$, $K = 2.0 \times 10^9 \text{ N/m}^2$ (Poisson's ratio $\nu = 0.4997$) and $\rho_0 = 1050 \text{ kg/m}^3$, so that in the undeformed configuration the elastic wave speeds for shear and pressure waves in the material are $c_T = 32.07 \text{ m/s}$ and $c_L = 1381 \text{ m/s}$, respectively. The effects of material non-linearities are investigated by considering three different values of J_m , $J_m = 0.5, 2.0, \infty$. Note that, at the limit of $J_m \rightarrow \infty$, the strain energy density function (1) reduces to that of a Neo-Hookean material [22, 24]. In Fig. 2 the

material response under uni-axial loading is reported in terms of the nominal stress S , normalized by G , versus the uni-axial deformation stretch. The results clearly indicate that smaller values of J_m introduce stronger non-linearities in the material behavior.

It is well known that, under compression, the geometric pattern of soft phononic crystals can suddenly change due to either: (a) microscopic instabilities with a spatial periodicity comparable to the size of the unit cell; or (b) macroscopic instabilities with a spatial periodicity much larger than the size of the unit cell [22, 25–28]. In this study, we investigate both instabilities of the phononic crystal under equi-biaxial compression, so that the macroscopic deformation gradient $\bar{\mathbf{F}}$ is given by

$$\bar{\mathbf{F}} = \lambda(\mathbf{e}_1 \otimes \mathbf{e}_1 + \mathbf{e}_2 \otimes \mathbf{e}_2), \quad (2)$$

where λ denotes the macroscopically applied stretch. We note that the undeformed configuration is characterized by $\lambda = 1$. Moreover, $\lambda > 1$ and $\lambda < 1$ represent the tension and compression load, respectively.

For the considered periodic structure, the onsets of both microscopic and macroscopic instabilities are detected by studying the response of a single unit cell (indicated by the dashed red square in Fig. 1A) along the loading path (2) for $\lambda < 1$ [22]. For all the cases considered here (i.e. $J_m = 0.5, 2.0, \infty$) a microscopic instability is detected at $\lambda_{cr}^{Micro} = 0.984$, while the onset of macroscopic instability occurs at $\lambda_{cr}^{Macro} = 0.961$. Therefore, microscopic instabilities are always critical in compression, leading to an enlarged representative volume element of 2×2 primitive unit cells and to the formation of a pattern of alternating, mutually orthogonal and elongated

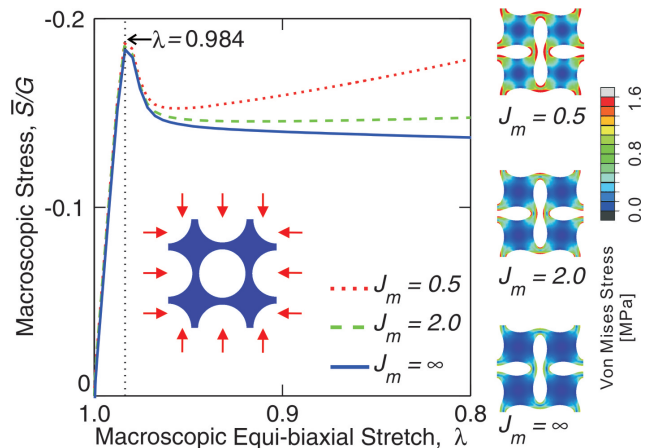


Figure 3: Macroscopic nominal stress vs stretch curves for the square array of circular holes in a Gent matrix. The departure from linearity is the result of an elastic instability that triggers the pattern transformation. The Von Mises stress distributions in the phononic crystals at $\lambda = 0.8$ are shown on the right for $J_m = 0.5, 2.0$ and ∞ .

holes (Fig. 1B).

The post-buckling response of the phononic crystal is then simulated by introducing small random imperfections in the initial geometry [22]. In Fig. 3 we present the static response of the phononic crystal for the three considered values of J_m in terms of the macroscopically effective nominal stress \bar{S} versus the applied stretch λ . Although the onset of instability is found not to be affected by J_m , we can clearly see that J_m has a strong influence on the postbuckling response of the structure.

To highlight the effect of the applied deformation on the propagation of elastic waves, we present in Fig. 4 the band structure and directionality diagrams of a phononic crystal made of a Gent material with $J_m = 0.5$ in both the undeformed ($\lambda = 1.0$, Fig. 4A) and deformed ($\lambda = 0.8$, Fig. 4B) configurations.

Figs. 4C and 4D show the band diagrams of the undeformed and deformed configurations, respectively. The dimensionless frequency $\tilde{f} = \omega a / (2\pi c_T)$, with a denoting the characteristic size of the unit cell in the undeformed configuration (Fig. 1A), is plotted as a function of the wave vector in the reciprocal space [22]. In the undeformed configuration, the periodic structure features a bandgap at $\tilde{f} = 0.61 \sim 0.82$. It is clear from Fig. 4D that the compression significantly alters the band structure. The pre-existing bandgap is shifted and widened to $\tilde{f} = 0.84 \sim 1.29$. In addition, a new bandgap that does not exist in the reference state is opened at $\tilde{f} = 0.50 \sim 0.64$.

To investigate the effect of deformation on the preferential directions of wave propagation, we focus on the low frequency range and calculate both phase velocity and group velocity for all directions of propagation at $\tilde{f} = 0.05$ (horizontal red line in Figs. 4C and 4D) [22]. In Figs. 4E and 4F we report the phase velocity profiles and in Figs. 4G and 4H the group velocity profiles for the undeformed and deformed configurations, respectively. In these plots all the wave velocities are normalized, so that the magnitude of maximum velocity, v_{max} , of any mode in any configuration is unity. It is important to note that the wave directionality in the low frequency range cannot be fully captured just by inspecting the band diagrams [12]. In fact, although the dispersion curves at low frequency resemble straight lines, which seem to imply linear dispersion relations, the approximation of an effective non-dispersive media is not applicable here, as phase and group velocities may exhibit very different directional behaviors [12].

We start by noting that, in the undeformed configuration, the phase velocity shows a preferred direction

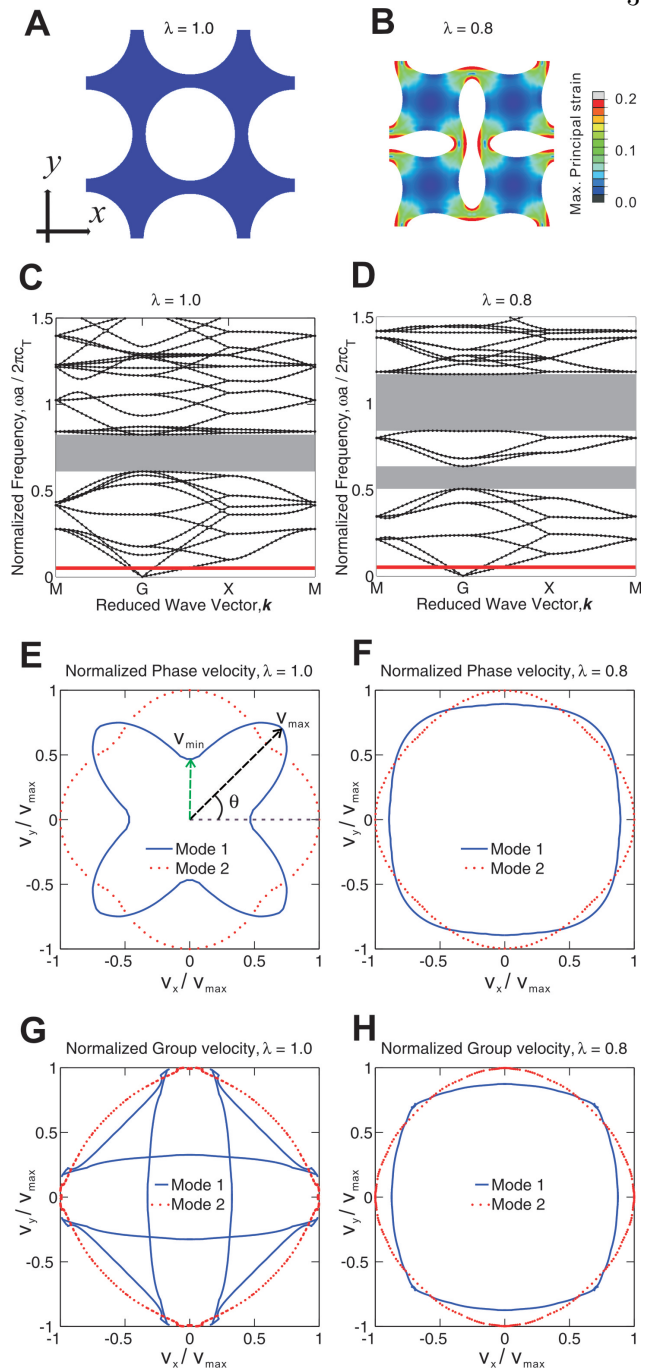


Figure 4: Dynamic response of the phononic crystal in the undeformed (left column, $\lambda = 1.0$) and deformed (right column, $\lambda = 0.8$) configuration. The effects of deformation on the bandgaps (B and C) and directionality of phase (D and E) and group (F and G) velocities are investigated.

of propagation at $\theta = 45^\circ$ for mode 1 (shear-dominated mode) and at $\theta = 0^\circ$ for mode 2 (pressure-dominated mode) (Fig. 4E). Moreover, the group velocity in the undeformed configuration exhibits two preferred directions at $\theta = 10^\circ$ and 80° for mode 1 (Fig. 4G), whereas it does not show a significant preferential direction of propagation for mode 2. Interestingly, the deformed configuration does not exhibit any strong preference in directions for both phase and

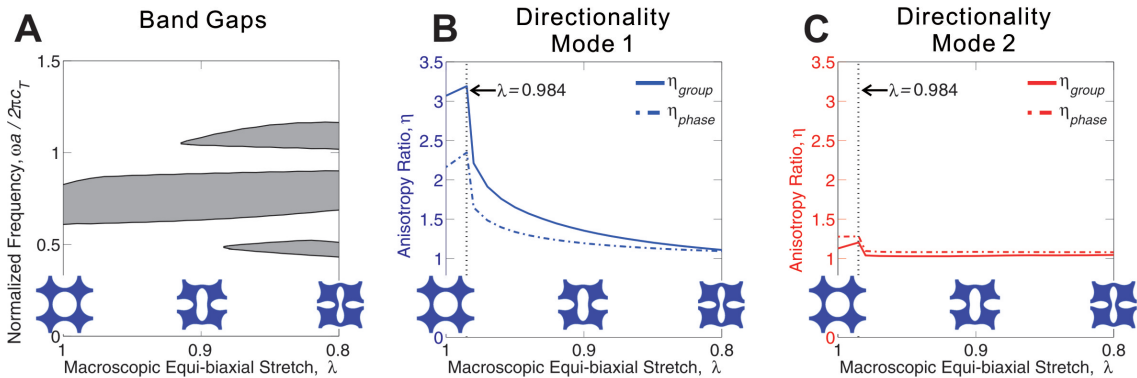


Figure 5: Effects of geometric non-linearities on (A) bandgaps and directionality of (B) mode 1 and (C) mode 2.

group velocities in both modes (Figs. 4F and 4H), so that it behaves as a nearly-isotropic medium. These results clearly indicate that the deformation have a significant effect on the wave directionality. Finally, we observe that the applied deformation has a more pronounced effect on the phase and group velocity profiles of mode 1 (shear-dominated mode), whereas the directionality of mode 2 (pressure-dominated mode) is only marginally affected.

The results presented above clearly show that the applied deformation strongly affects not only the static, but also the dynamic response of phononic crystals. However, to design the next generation of tunable phononic crystals that take full advantage of the changes on the dynamic response induced by the applied deformation, this mechanism needs to be thoroughly understood. While it is well known that the applied deformation introduces both geometric and material non-linearities, it is not clear how these two effects control the tunable dynamic response of the phononic crystal. To gain knowledge on this front, we numerically investigate the separate effects of (I) geometric and (II) material non-linearities on both the bandgaps and wave directionality.

Geometric non-linearities. To evaluate the effect of geometric non-linearities on the dynamic response of the phononic crystal, we investigate the propagation of elastic waves in a stress-free structure with the deformed geometry (i.e. the shape of the structure is determined by the post-buckling analysis). More specifically, we compress the structure up to a certain value of λ and then set the all the components of the stress to zero before performing the wave propagation analysis. Thus, the inhomogeneous stress distribution is not taken into the consideration when computing the dynamic response.

The evolution of the bandgaps as a function of λ is shown in Fig. 5A. The change in geometry induced by the applied deformation is found to shift and widen the main bandgap and to generate two additional bandgaps, one higher and the other lower than the

main gap, which open at $\lambda = 0.92$ and $\lambda = 0.88$, respectively. These deformation-induced bandgaps also shift and widen for decreasing values of λ . Finally, we note that these results are independent of J_m , since, in order to investigate the geometric effects alone, we have neglected the stress distribution in the deformed configuration (note that the incremental response for an unstressed Gent material is independent of J_m).

To describe the evolution of the directionality of propagating waves, we define the anisotropy ratio:

$$\eta = \frac{v_{max}}{v_{min}}, \quad (3)$$

where v_{max} and v_{min} are the maximum and minimum wave velocities, respectively (see Fig. 4E). The trends of η for both phase velocity and group velocity of mode 1 (shear-dominated mode) and mode 2 (pressure-dominated mode) as a function of λ are reported in Figs. 5B and 5C, respectively.

For mode 1, the anisotropy ratios of both the group and phase velocity profiles (η_{group} and η_{phase}) rise from the initial values up to a turning point, then to rapidly decrease as function of λ and approach unity (Fig. 5B). Note that the turning point at $\lambda = 0.984$ corresponds to the onset of structural instability. Similar trends are observed for mode 2 (Fig. 5C), but the changes induced by deformation are less dramatic in this case. In summary, the results from both modes show that the geometric non-linearities induced by instability have a significant effect on the wave directionality; They remove the directional characteristics of both modes and make the wave propagation more isotropic.

Material non-linearities It is apparent from Fig. 4B that deformation not only affects the geometry, but also induces an inhomogeneous strain/stress distribution within the phononic crystal. Substantial stress concentrations are developed during compression and they strongly depend on the non-linear material response, which is characterized by J_m (Fig. 3).

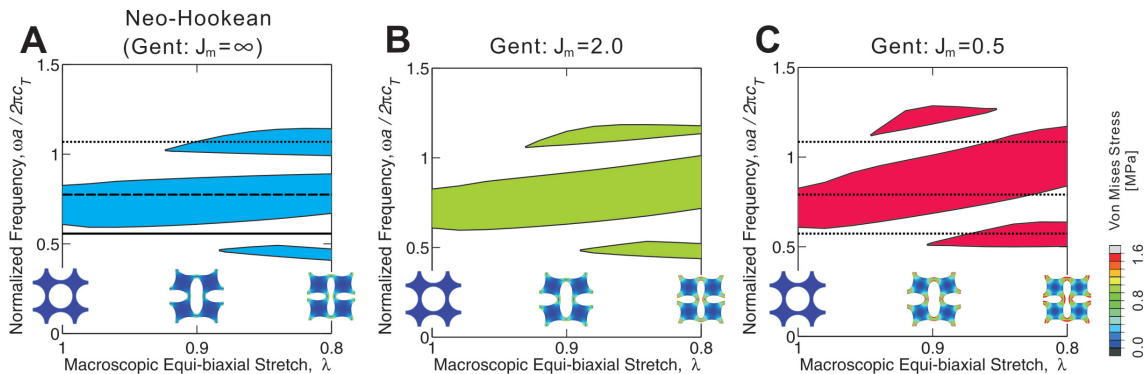


Figure 6: Effects of material non-linearities on the bandgaps. Soft phononic crystals made of Gent materials with (A) $J_m = \infty$, (B) $J_m = 2.0$ and (C) $J_m = 0.5$ are investigated.

To investigate the effect of material non-linearities on the propagation of elastic waves, we start by studying the response of a phononic crystal made of a Neo-Hookean material (i.e. Gent material with $J_m = \infty$). The response of such material is weakly non-linear and the stiffening effect induced by the applied deformation is negligible in this case. In Fig. 6A, we report the evolution of the bandgaps as a function of the applied deformation λ . Comparison between Figs. 5A and 6A reveals that the dynamic response of the phononic crystal is not affected by the inhomogeneous stress state. Therefore, for a phononic crystal made of an Neo-Hookean elastomeric material, the geometric non-linearities induced by the applied deformation fully control the position and width of the bandgaps.

Next, we investigate the evolution of the bandgaps for phononic crystals made of elastomers with stronger material non-linearity. As shown in Fig. 2, smaller values of J_m introduce stronger material non-linearities under the applied deformation. Here, we comparatively study the cases of phononic crystals made of Gent materials with $J_m = 2.0$ and 0.5 (Figs. 6B and 6C). We notice that in both cases the bandgaps are significantly affected by material non-linearities when $\lambda < 0.9$. We find that smaller values of J_m provide a larger range of tunability for the bandgaps. To better quantify the effect of material non-linearity on the bandgap tunability, we divide the wave frequencies into three categories: (i) frequencies that are always in the propagating band (e.g. $\tilde{f} = 0.55$, continuous horizontal line in Fig. 6A); (ii) frequencies that are always in the bandgap (e.g. $\tilde{f} = 0.75$, dashed horizontal line in Fig. 6A); and (iii) frequencies that can be switched on / off by the applied deformation (e.g. $\tilde{f} = 1.05$, dotted horizontal line in Fig. 6A). We start by noting that all the three frequencies highlighted in Fig. 6A turn into category (iii) when $J_m = 0.5$ (see dotted horizontal lines in Fig. 6C). In fact, for $J_m = 0.5$, the frequencies in the entire region $\tilde{f} = 0.49 \sim 1.28$ can be switched on / off by the applied deformation. Therefore, since large regions

of type (iii) frequencies are desirable for the design of a highly tunable system, our results indicate that phononic crystals made of materials with stronger non-linearities can offer enhanced bandgap tunability.

To further study the effect of the material parameter J_m on the bandgaps, we calculate the relative size of the band-gaps as the ratio between gap width and the mid-gap position,

$$\Delta\omega_{relative} = \frac{\omega_{upper} - \omega_{lower}}{(\omega_{upper} + \omega_{lower})/2}, \quad (4)$$

where ω_{upper} and ω_{lower} are the frequencies of upper and lower edge limits of a bandgap, respectively. It has been previously shown that the relative size defined above is an important design parameter, and that a large relative size of the bandgap is preferable for many applications [4]. The evolution of $\Delta\omega_{relative}$ as a function of the applied deformation is reported in Figs. 7A, B and C for the first, second and third bandgap, respectively. The responses of phononic crystals made of Gent material with $J_m = 0.5, 1.0, 2.0, 5.0, 10.0$ and ∞ are considered. For all different materials considered here and for all three bandgaps $\Delta\omega_{relative}$ is found first to increase as a function of the applied deformation, then to reach a maximum and finally either to plateau or slightly decrease. For instance, in the case of $J_m = 0.5$, $\Delta\omega_{relative}$ reaches the maximum value at $\lambda = 0.83, 0.94$ and 0.91 for the first, second and third bandgaps, respectively. We note that the decrease of $\Delta\omega_{relative}$ after its maximum is due to the fact that the position shifting effect is stronger than the widening effect. That is, in Eqn. (4), the increase in the denominator becomes faster than the increase in the numerator. As a result, although the bandgap keeps widening upon further deformation, $\Delta\omega_{relative}$ diminishes. This feature described above becomes more pronounced when the applied deformation is large and the constituting material is highly non-linear.

Finally, our analysis also reveals that material non-linearities do not affect the directionality of the propagating waves at low frequency. The velocity

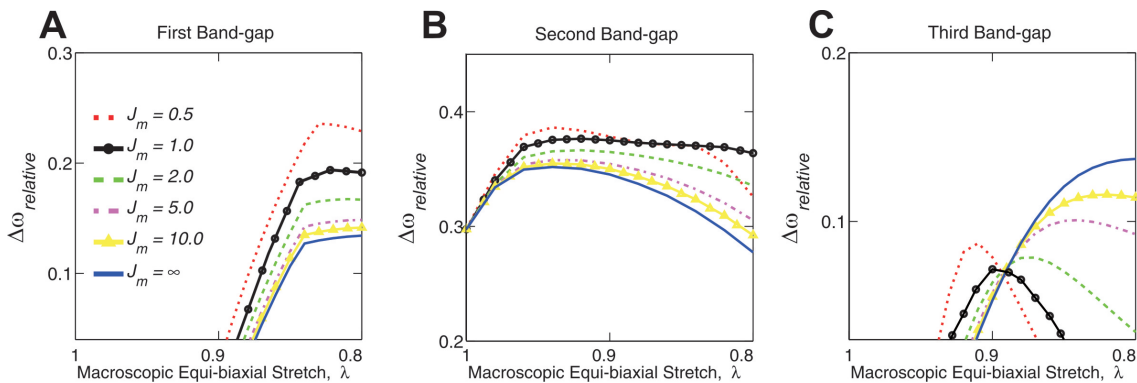


Figure 7: Comparison of the change of relative bandgaps during deformation

profiles obtained for a phononic crystal made of Gent material with $J_m = \infty$, 2.0 and 0.5 are found to be the same as those shown in Figs. 5B and 5C. Therefore, these results suggest that only changes in geometry can be effectively used to tune the directional characteristics of the lower bands.

To summarize, we use numerical simulations to study the propagation of small-amplitude elastic waves in highly deformed phononic crystals and investigate the effect of deformation on bandgaps and directionality of propagating waves. The contributions of geometric and material non-linearities to the tunable response of phononic crystals are revealed. The bandgaps are found to be affected both by geometric and material non-linearities, while the directional preferences of the wave modes in low passing bands are shown to be sensitive only to changes in geometry. Enhanced tunability of the bandgaps is found for phononic crystals made of materials with stronger non-linear behavior. Finally, the changes in geometry introduced by the applied deformation gradually remove the directional characteristics of the lower propagation modes, making the wave propagation more isotropic. The results presented in this paper provide useful guidelines for the design of tunable phononic devices.

ACKNOWLEDGEMENTS

This work has been supported by Harvard MR-SEC through grant DMR-0820484 and by NSF through grants CMMI-1120724 and CMMI-1149456 (CAREER). K.B. acknowledges start-up funds from the Harvard School of Engineering and Applied Sciences and the support of the Kavli Institute and Wyss Institute at Harvard University.

- [1] M. Sigalas and E. Economou, *Solid State Communications* **86**, 141 (1993), ISSN 0038-1098.
- [2] M. S. Kushwaha, P. Halevi, L. Dobrzynski, and B. Djafari-Rouhani, *Phys. Rev. Lett.* **71**, 2022 (1993).
- [3] M. Ruzzene and F. Scarpa, *Phys. Sta. Sol. B* **242**, 665 (2005).
- [4] M. Maldovan and E. Thomas, *Applied Physics B* **83**, 595 (2006), ISSN 0946-2171.
- [5] K. Bertoldi and M. C. Boyce, *Phys. Rev. B* **78**, 184107 (2008).
- [6] J. O. Vasseur, A. Hennion, B. Rouhani, F. Duval, B. Dubus, and Y. Pennec, *J. App. Phys.* **101**, 114904 (2007).
- [7] W. Cheng, J. J. Wang, U. Jonas, G. Fytas, and N. Stefanou, *Nat. Mater.* **5**, 830 (2006).
- [8] F. Casadei, L. Dozio, M. Ruzzene, and K. Cunefare, *J. Sound. Vib.* **329**, 3632 (2010).
- [9] F. Casadei, B. Beck, K. A. Cunefare, and M. Ruzzene, *Int. J. Solids Struc.* **23**, 1169 (2012).
- [10] M. Ruzzene, F. Scarpa, and F. Soranna, *Smart. Mater. Struct.* **12**, 363 (2003).
- [11] M. Collet, M. Ouisse, M. Ruzzene, and M. N. Ichchou, *Int. J. Sol. Struct.* **48**, 2837 (2011).
- [12] F. Casadei and J. Rimoli, *International Journal of Solids and Structures* pp. – (2013), ISSN 0020-7683.
- [13] E. Nolde, R. Craster, and J. Kaplunov, *Journal of the Mechanics and Physics of Solids* **59**, 651 (2011).
- [14] S. Gonella and M. Ruzzene, *International Journal of Solids and Structures* **45**, 2897 (2008).
- [15] S. Gonella and M. Ruzzene, *Journal of Sound and Vibration* **312**, 125 (2008).
- [16] Vasseur, J. *Phys. Condensed Mat.* (1994).
- [17] Zhou, *J. App. Phys.* (2009).
- [18] Movchan, *Mat. Sci. Eng.* (2006).
- [19] M. Maldovan and E. Thomas, *Periodic Materials and Interference Lithography for Photonics, Phononics and Mechanics* (Wiley-VCH, 2009).
- [20] J. Jang, C. Koh, K. Bertoldi, M. Boyce, and E. Thomas, *Nano Letters* **9**, 2113 (2009).
- [21] L. Wang and K. Bertoldi, *International Journal of Solids and Structures* **49**, 2881 (2012).
- [22] See Supplementary Material at [URL] for the details of the general formulation and numerical procedures.
- [23] A. Gent, *Rubber Chem. Tech.* **69**, 59 (1996).
- [24] L. Treloar, *Trans. Faraday Soc.* **40**, 59 (1944).
- [25] G. Geymonat, S. Muller, and N. Triantafyllidis, *Arch. Ration. Mech. Anal.* **122**, 231 (1993).

- [26] N. Triantafyllidis, M. D. Nestorovic, and M. W. Schraad, *J. Appl. Mech.* **73**, 505 (2006).
- [27] K. Bertoldi, M. Boyce, S. Deschanel, S. M. Prange, and T. Mullin., *J. Mech. Phys. Solids* **56**, 2642 (2008).
- [28] Overvelde, S. Shan, and K. Bertoldi, *Adv. Mat.* (2012).